Dynamics of the extratropical response to a tropical Atlantic SST anomaly

Shuanglin Li[1], Walter A. Robinson[2], Martin P. Hoerling[1], and Klaus M. Weickmann[1]

(1) NOAA Earth System Research Laboratory, Boulder, Colorado

(2) Department of Atmospheric Sciences, University of Illinois, Urbana, Illinois

Submitted to J. Climate on December 22, 2005

Revised on 15 June 2006

Corresponding author address:

Dr. Shuanglin Li, NOAA ESRL-CIRES CDC, R/PSD1, 325 Broadway, Boulder, CO 80305-3328

E-mail: shuanglin.li@noaa.gov

Abstract

Previous atmospheric general circulation model (AGCM) experiments revealed that atmospheric responses to a tropical Atlantic sea surface temperature anomaly (SSTA) were asymmetric with respect to the sign of the SSTA. A positive SSTA produced a south-north dipole in geopotential heights, much like the North Atlantic Oscillation (NAO), while a negative SSTA yielded an eastward propagating wave train, with the northern lobe of the NAO absent.

Here these height responses are decomposed into components that are symmetric or antisymmetric with respect to the sign of the SSTA. The symmetric, or notionally linear, component is a nearly south-north dipole projecting on the NAO, while the antisymmetric, or notionally nonlinear, component is a different dipole. Experiments with a diagnostic linear baroclinic model (LBM) suggest both components are maintained primarily by transient-eddy forcing. Dynamical mechanisms for the formation of the two components are explored using the LBM and a nonlinear barotropic vorticity equation model (BVM). Transient-eddy feedback is sufficient to explain the linear response. The NAO-like linear response occurs when the initial heating induces transient-eddy forcing in the exit of the Atlantic jet. The structure of the background absolute vorticity in this region is such that this transient-eddy forcing induces a nearly north-south dipole in anomalous geopotential heights. When the nonlinear self-interaction of this transient-induced low-frequency perturbation is included in the BVM, the dipole axis tilts to the east or west, resulting in a response that is nonlinear about the sign of the forcing.

1. Introduction

Forcing of the extratropical atmosphere by anomalous sea-surface temperatures (SSTA), especially in the tropics, can generate potentially predictable variability on timescales – seasonal to decadal – which cannot arise from internal atmospheric processes alone. Thus it is of both practical and scientific interest to understand, in some detail, how the extratropical atmosphere responds to such forcing. The extratropical response is conventionally estimated from the difference between the seasonal mean circulation when the tropical ocean is warmer than usual relative to when the tropical ocean is cooler (e.g., van Loon and Rogers 1981), or as the linear regression of circulation anomalies against an SSTA index (Horel and Wallace 1981). Implicit in these approaches is the assumption that the atmospheric response is approximately linear. Responses in atmospheric general circulation models (AGCMs), however, exhibit considerable nonlinearity (Kushnir et al. 2002), with respect to the sign of forcing (e.g., Pitcher et al. 1988; Kushnir and Lau 1992; Drevillon et al. 2003; Peng et al. 2002; 2003; Magnusdottir et al. 2004; Lin and Derome 2004), and with respect to the spatial structure of forcing (e.g., Sutton et al. 2000; Robinson et al. 2003; Deser et al. 2004). These nonlinearities were denoted "sign nonlinearity" and "additive nonlinearity", respectively, by Robinson et al. (2003). An atmospheric response can be separated into two components, the linear and the nonlinear. The structures of these components are usually different, and they may arise from different dynamics.

Two mechanisms have been invoked to explain the linear response: wave propagation and transient-eddy feedback. Planetary wave propagation accounts for the "Pacific-North American (PNA)" linear response to El Niño/ La Niña SST forcing (Hoskins and Karoly 1981; Simmons 1982). It may play a role in the formation of the North Atlantic Oscillation (NAO) (Branstator 2002). Transient-eddy feedback can be understood as comprising several steps (Lau and Nath 1991;

Lin and Derome 1995; Peng and Whitaker 1999; Peng et al. 2003, hereafter PRL03): the tropical heating anomaly initially induces a thermally forced quasi-stationary disturbance that propagates into the extratropics. This anomalous flow acts on the stormtrack, modulating the organization of synoptic eddies and inducing anomalies in the transient-eddy forcing of the time-averaged flow. The anomalous transient-eddy modifies the initial heating-induced response, and the resulting changes in the quasi-stationary flow further influence the eddies. Through this interaction, the transient-eddy induced component of the quasi-stationary anomaly tends to be reinforced while the component directly induced by anomalous heating may be damped. When direct responses to the heating and to the transient feedback are weak, each step in this process is predominantly linear. Thus, the eddy-feedback mechanism can explain essence of the linear response.

Nonlinearity can arise from both thermodynamics and dynamics. Thermodynamically, a "built-in" nonlinearity exists in the bulk formulae for the sensible and latent heating fluxes at the sea surface, due to the quasi-exponential dependence of saturation vapor pressure on temperature and the multiplicative dependence of heat and momentum fluxes on the surface wind speed. Also, tropical convection and rainfall depend on the full SST, rather than the SST anomaly. This nonlinearity contributes to the asymmetric atmospheric response about the sign of the SSTA in the eastern equatorial Pacific (Hoerling et al. 1997; Hoerling and Kumar 2002). Dynamically, the direct extratropical response to tropical thermal forcing alters the midlatitude flow and modifies the propagation of stationary waves. The direct response can also affect the position of the subtropical critical line, thereby influencing the reflection of planetary waves (Robinson et al. 2003). Finally, in the eddy-feedback mechanism, nonlinearity can be induced when the thermal or transient-eddy forcing are sufficiently strong. This was confirmed by PRL03, in addressing the nonlinear response

to the North Atlantic SST tripole, and also by Lin and Derome (2004) in their study of the nonlinear responses to El Niño/ La Niña.

Significant sign-nonlinearity was found in recent AGCM studies of the influence of North Atlantic SSTA on the NAO. The NAO is the leading pattern of variability over the North Atlantic in winter over a broad range of timescales. Its formation is primarily attributed to the processes internal to the atmosphere, especially the interaction of synoptic eddies with the quasi-stationary flow. A reasonable null hypothesis is that the NAO is driven entirely by processes internal to the atmosphere, and with any longer term variations appearing as a consequence of sampling, or "climate noise" (Feldstein 2000). This is supported by the fact that NAO-like fluctuations emerge in AGCM experiments forced with the climatological SSTs (e.g., Barnett 1985; Saravanan 1998), This null hypothesis cannot, however, account for decadal variations in the NAO alone, such as its increasing trend over the second half of the 20th century (e.g., Hoerling et al. 2001). An alternative hypothesis is that the NAO is modulated by the underlying ocean on seasonal to decadal timescales. This alternative hypothesis drives the recent interest in the possible influence of the SST (e.g., Sutton et al. 2000; PRL03) or of air-sea coupling on the NAO (e.g., Peng et al. 2005, hereafter PRLH; Li et al. 2006a, b). Observational analyses suggest at least two Atlantic SST patterns are linked to the NAO. One is the North Atlantic tripole, the leading pattern of wintertime SST variability linearly related to the NAO (see PRL03). The other is a Pan-Atlantic SSTA pattern (Czaja and Frankignoul 2002, hereafter CF02), comprising the extratropical "Horseshoe", with warm waters southeast of Newfoundland surrounded by cold waters on the east side of the Atlantic, and an equatorial warm anomaly (see Fig. 2 in CF02; also Fig. 1 in PRLH). CF02 found that the pan-Atlantic SST pattern leads the wintertime NAO by up to four months.

Whether the SST tripole can induce the NAO was addressed in AGCM experiments (e.g., Sutton et al. 2000). PRL03 addressed this problem in 100-member ensembles using a version of the NCEP (National Centers for Environmental Prediction) atmospheric seasonal prediction model (Kanamitsu *et al.* 2002), with T42 spectral truncation and 28 sigma levels. Two sets of experiments were performed, applying the tripole SSTA added to or subtracted from the seasonally varying SST climatology. The model responses exhibit asymmetry with respect to the sign of the forcing: a wave-like response to the positive tripole and a negative NAO-like response to the sign-reversed tripole. The linear (sign symmetric) component of the response is NAO-like, whereas the nonlinear (sign antisymmetric) component is a dipole tilted to the NE, with its positive lobe over Iceland and its negative lobe over Iberia. Experiments with a linear baroclinic model (LBM) and a statistical stormtrack model (STM) revealed that the aforementioned eddy-feedback mechanism was the dominant source of the linear response. The nonlinear response was also studied using the LBM and STM, modifying their basic states to include the influence of heating- or transient-induced quasi-stationary perturbation. The results reveal that the self-interaction of the quasi-stationary response to diabatic heating is the primary source of the nonlinear response, although it is reinforced by transient eddy feedback.

AGCM studies have also addressed the NAO response to the pan-Atlantic SSTA (e.g., Drevillon et al. 2003). PRLH performed ensemble experiments, forcing the same NCEP AGCM with the extratropical (Horseshoe pattern) or the tropical component (shading in Fig. 1d here) of the pan-Atlantic SSTA. The response to the Horseshoe pattern is baroclinic, with little projection on the NAO. In contrast, the tropical portion of the pan-Atlantic SSTA produced a robust NAO response. The response to the tropical forcing is nonlinear with respect to its sign. In late winter (February-April) a positive tropical anomaly induces a negative NAO, while the response to a

negative anomaly is a wavetrain (Fig. 1, also Fig. 8 of PRLH), which is even more significant through the whole cold season (October-April) (not shown).

Here we extend the results of PRLH, by addressing the atmospheric dynamics of the response to tropical Atlantic SST forcing. We focus on the role of transient eddy feedback in generating the NAO, and on the sources of nonlinearity in the response. For the linear response, following PRL03, we perform a sequence of linear model experiments. These confirm the importance of the eddy-feedback mechanism. A more detailed diagnosis of the dynamics reveals that only transient forcing located in the jet exit contributes to the NAO response. This can be attributed to the structure of background vorticity around the jet exit. For nonlinear response, we use a nonlinear barotropic vorticity equation model (BVM), the results of which indicate that the self-interaction of the response to eddy forcing is the principle source of nonlinearity. The paper is organized as follows. Section 2 introduces the diagnostic models. In section 3, the maintenance of the linear and nonlinear components of the response is diagnosed using LBM experiments. In section 4, the formation of these two components is investigated through LBM and BVM experiments. The final section includes a summary and discussions of the results.

2. Diagnostic tools

2.1 *Linear Baroclinic Model (LBM)*

In atmospheric circulation studies, it is often desirable to diagnose the relative importance of various forcings, such as anomalous diabatic heating and the convergence of the transient-eddy vorticity flux, in maintaining a quasi-steady anomalous flow, or to determine the direct response to a specific forcing. This can be accomplished using a linear model. There are two alternative approaches to obtain steady linear model solutions. One is to invert the linear model operator, as in

Ting and Lau (1993). The other is to integrate a time-dependent linearized model until a steady response is reached, as in Peng and Whitaker (1999).

The present LBM is the same as that used by Peng and Whitaker (1999). It is a time-dependent spectral model with a horizontal resolution of T21 and 10 equally spaced pressure levels. No topography is prescribed. The linearization is about a three-dimensional time-mean flow. The model treats the diabatic heating and the transient-eddy flux of vorticity as forcings. The basic state is the February-April mean of 100 AGCM control run. Rayleigh friction and Newtonian damping have rates of $(1 \text{ day})^{-1}$ at the lowest level and $(7 \text{ days})^{-1}$ at other levels. Biharmonic horizontal diffusion with a coefficient of 2×10^{16} m^4s^{-1} is applied everywhere, and Fickian thermal diffusion with a coefficient of 2×10^6 m^2s^{-1} is included to represent the heat fluxes by transient eddies. With these values for dissipation and diffusion, the different basic states are stable, and a steady response to a forcing is reached after about 30 days. Averages over the final 5 days of 30-day integrations are used to approximate the steady linear responses.

2.*2 Storm Track Model (STM)*

There is a two-way interaction between the time-mean flow and synoptic-scale eddies (e.g., Branstator 1992). On one hand, anomalous eddy activity induces a time-mean flow anomaly, which can be estimated using the LBM described above. On the other hand, a time-mean flow anomaly will modulate the organization of synoptic eddies, and result in anomalies in the transient-eddy forcing. Various approaches have been taken to estimate the transient-eddy responses to an anomalous flow (see references in PRL03). We use the same statistical storm-track model (STM) developed in PRL03. It is constructed by performing a multiple linear regression of the anomalous transient-eddy forcing against the anomalous time-mean flow. The time-mean flows are the

February-April monthly mean geopotential heights, and the transient-eddy forcing is the streamfunction tendency, also monthly means, due to the transient-eddy vorticity flux. Transient eddies are defined as those with time scales less than 9 days. The regression is performed using output from the AGCM control runs north of 20^{o}N and using the 40 leading EOFs of both fields.

2.3 *Barotropic Vorticity Equation Model (BVM)*

A nonlinear barotropic model is used to diagnose the mechanisms that lead to nonlinearity in the responses to tropical forcing. The use of a barotropic model for this purpose is supported by the equivalent barotropic nature of the responses (Fig. 1b and f). Our barotropic vorticity model (BVM) is formed by adding linear damping and additional forcing to the barotropic model used by Held and Phillips (1987). A detailed description is available in the documentation for the dynamical core of the Geophysics Fluid Dynamical Laboratory (GFDL) Flexible Model System (FMS, www.gfdl.noaa.gov/~fms/). The model equation is,

$$\frac{\partial \zeta}{\partial t} = -J(\psi, f+\zeta) - \gamma \nabla^8 \zeta - \lambda \zeta + F'_\zeta \qquad (1).$$

This equation is resolved in spectral space at a triangular 85 (T85) truncation. The diffusion coefficient, γ, is 1.0x10^4 m^{8}s^{-1}, and the linear damping coefficient, λ, is 2.0x10^{-6}s^{-1}, corresponding to an e-folding time of 5.8 days. The model time step is 20 minutes. With these values for dissipation, a steady response to an external forcing is achieved after 30 days. Thus, the model is integrated for 50 days, and the average solution from days 31 through 50 represents the equilibrium response. The model uses the February-April 300-hPa basic state derived from the AGCM control runs. The vorticity forcing needed to maintain the AGCM climatological zonally asymmetric flow is constructed so that the AGCM climatological flow is an exact solution of the BVM. This forcing is obtained by calculating the vorticity tendency over a single time step when the BVM is

initialized with the AGCM climatology. The forcing is then given by –1 times the resulting tendency. The BVM response to additional forcing is then the difference between the equilibrium responses with and without this additional forcing added to the climatological forcing.

3. Maintenance of the linear and nonlinear responses

Hereafter, the ensemble time-mean flow in the AGCM experiments with a positive or negative SSTA is denoted <P> and <N>, and that with the climatological monthly SST (the control experiments) is denoted <C>. Thus, the modeled atmospheric responses to the positive and negative SSTA are <P>-<C> and <N>-<C>. The symmetric response with respect to the sign of the SSTA includes any linear response, whereas any response that is antisymmetric with respect to the sign of the SSTA is necessarily nonlinear. Therefore, following PRL03 and Drevillon et al. (2003), the linear component of the response to this SSTA is approximated by <L> = (<P> - <N>)/2, and the nonlinear component is approximated by <NL> = [(<P> - <C>) + (<N> - <C>)]/2. It should be kept in mind, however, that <L> includes any response that varies with an odd power of the SSTA, and need not be strictly linear.

Figure 2a and d show the linear and nonlinear AGCM 500-hPa height responses. The linear response (Fig. 2a) resembles the NAO, while the nonlinear component (Fig. 2d) is a different dipole, which is more obvious in the response through the whole cold season, October-April (not shown). The response to the positive SSTA (Fig. 1a) more closely resembles the linear response than that to the negative SSTA (Fig. 1e). The linear and nonlinear components of 300-hPa transient forcing (Fig. 2c and f) largely resemble the corresponding components of 500-hPa height response (Fig. 2a and d).

Anomalous transient-eddy vorticity forcing and diabatic heating are the primary forcings that maintain quasi-steady atmospheric anomalies (e.g., Branstator 1992; Lau and Nath 1991; PRL03). To calculate the transient-eddy vorticity forcing, a "poor man" filter is used to isolate motions with time scales less than 9-days (PRL03; Li 2004). Anomalous diabatic heating is calculated from six diabatic heating variables from the AGCM daily output, i.e., the large-scale condensational heating, heating by deep and shallow convection, heat transport by vertical diffusion, and long-wave and solar radiative heating. The horizontal distribution of the total anomalous heating is largely captured by the anomalous precipitation. The February-April mean anomalous transient-eddy forcing for the positive and negative SSTA cases (Fig. 1c and g) exhibits a similar asymmetry with respect to the sign of the SSTA, as do the geopotential responses (Fig. 1a and e). In contrast, the precipitation anomalies are nearly symmetric about the sign of the SSTA (Fig. 1d and h). The anomalous transient forcing and diabatic heating are interpolated to the 10 equally-spaced pressure levels and the T21 horizontal grids of the LBM. The separate contributions of these two forcings to maintaining the AGCM response are analyzed using the LBM. The summed LBM response to the two forcings largely reproduces the AGCM response, albeit with a weaker amplitude, for these two SSTA cases (Fig. 2b, e). As was discussed in PRL03, these weak amplitudes likely result from the limitation of the linear dynamics and from the differences between the AGCM and the LBM. Because the amplitude of the LBM response depends on the strength of the dissipation, that the spatial patterns obtained by the LBM and the AGCM are similar is most significant.

Comparing Fig. 2a and b shows that the linear component of the AGCM response is largely maintained by a combination of heating and transient eddy forcing, while Figs. 3a and b show that the transient-eddy forcing is more important, especially north of 40°N. For the nonlinear

component (Figs. 2d and e and Figs. 3c and d), transient-eddy forcing is more important almost everywhere. This is consistent with the evident asymmetry between the anomalous transient forcings (Fig. 1c and g, also Fig. 2f), but the lack of asymmetry between the anomalous precipitation for the opposite signs of SSTA (Fig. 1d and h). Overall, the transient-eddy forcing is more important than heating in maintaining both the linear and nonlinear responses to the tropical SSTA, consistent with what PRL03 found for the response to the North Atlantic tripole.

4. Origins of linear and nonlinear responses

4.1 Origin of the linear response

The modeled NAO-like linear response in Fig. 2a has a strength of about 20 mK^{-1} and a signal-noise ratio of about 20/65 =30%, given that the model's atmospheric internal variability, represented by the standard deviation of February-April monthly mean geopotential heights, is about 65 meters near the location of the strongest height response. Thus, in this model, and presumably in the atmosphere, variability in the NAO is primarily stochastic, even in the presence of significant SST anomalies. The relatively small SST response is of interest, however, because of its potential persistence and predictability. Here we explore the dynamics of that response using our linear model (LBM).

An idealized heating (Fig. 4a) is prescribed to represent the heating initially induced by the SSTA. It is designed to resemble the AGCM heating anomaly in early winter more than in late winter (cf. Fig. 10 in PRLH). The early winter heating anomaly may be less influenced by the extratropical circulation feedback because the extratropical response has not yet fully developed. This heating is stronger than that diagnosed from the AGCM experiments, in order to compensate for the weakness of responses in the LBM (see PRLH). Modest changes to its vertical profile or

horizontal shape have little effect on the structure of the resulting response. The LBM 300-hPa geopotential response (Fig. 4b) is wavetrain-like, similar to that obtained by PRLH (their Fig. 12). This is the direct linear response to tropical heating.

When this linear response acts on the storm track, it induces anomalous transient-eddy activity. Figure 4c shows the anomalous transient-eddy forcing – specifically the streamfunction tendency at 300-hPa due to transient-eddy vorticity fluxes – computed by applying the linear response shown in Fig. 4b to the storm-track model (STM). The response to this transient-eddy forcing (Fig. 4d), calculated by applying it to the LBM, reinforces the direct response to tropical heating. Moreover, it resembles the linear component of the AGCM response shown in Fig. 2a, with a strong projection on the NAO. When this feedback loop between eddy forcing and the linear response is carried through additional steps, using the STM to derive additional eddy forcing that is then applied to the LBM, the result (not shown) more closely resembles the NAO. Since both the LBM and the STM are linear models, the result of such an iterative procedure can explain only the linear part of the GCM response. The results suggest that this linear response is largely maintained by transient-eddy forcing. Thus, the eddy-feedback mechanism proposed by Peng and Whitaker (1999) applies to the present tropically forced response, as it did to the midlatitude SSTA case they considered.

4.2 Dynamics of linear dipolar response

The transient forcing in Fig. 4c comprises three centers of action, marked "S", "M", and "N" (for south, middle, and north) in the figure. A previous study of the effects of Pacific transient-eddy forcing (Li et al. 2006a) suggests that only forcing in the core of the jet exit induces a meridional dipole, while forcing elsewhere induces localized or wave-train responses. To explore

the generality of that result, we perform additional LBM experiments using the combined or separate components of the transient-eddy forcing. Figure 5a shows the response to the transient-eddy forcing in all three shaded regions in Fig. 4c. The forcing is applied only in regions over the Atlantic where the streamfunction tendency at 250-hPa is stronger than 1.5 m^2s^{-2}. The pattern of the response resembles that to the global transient-eddy forcing (cp. Fig. 5a with 4d), although, because some forcing is excluded, the amplitude is reduced by about 20%. Responses to each center are shown in Figs. 5b, c, and d. The main source of the dipolar response is the middle center, which is in the jet exit, while the other components do not contribute significantly to the dipole.

To investigate further whether forcing in the jet exit is critical for producing a dipole, additional LBM experiments are performed with idealized forcing centering in different locations, indicated by the dots in Fig. 6c. The strength of the idealized transient-eddy forcing is approximately five times that diagnosed from the AGCM responses. Such amplification should influence only the amplitude, not the pattern of the response in the LBM. Figures 6a and b show its vertical profile and spatial pattern, expressed as a stream-function tendency. These are based on the transient eddy forcing that arises in the AGCM. The results are insensitive to modest modifications in the shape and profile of the forcing. Fig. 7 displays examples of the responses to forcing in different locations. Only forcing in the jet exit, such as at (40^oN, 40^oW), induces a NAO-like dipolar response. Forcing elsewhere induces either a localized or a wave-train response. These results are consistent with the Pacific case discussed by Li et al. (2006a). One common response feature for all those forcing cases is the cyclonic negative height response downstream. The unique feature for the NAO-like dipole response is the anti-cyclonic positive height anomaly just north of the negative height response (Fig. 7e). Thus, understanding the formation of the northern lobe is the key to understanding the NAO-like responses.

Rossby-wave propagation depends on the advection of absolute (or potential) vorticity up or down its basic-state gradient by perturbation winds. When basic-state vorticity contours are zonal, linear Rossby waves must have a zonal component to their propagation, and purely meridional dipoles are impossible. Meridional dipoles can result either when the forcing is dipolar, which is not the case in Fig. 5c or Fig. 7e, or when the basic state vorticity contours deviate from zonality. Figure 8a shows the idealized forcing and the resulting geopotential height response, superimposed on the contours of basic state absolute vorticity, when the forcing is centered at (40°W, 40°N), while Fig. 8b shows a schematic of the response. Obviously the basic state absolute vorticity deviates strongly from zonality over the region of the NAO-like response. Whether this deviation contributes significantly to the formation of this northern lobe of the dipole can be determined from a diagnosis of the terms in the linearized vorticity equation.

$$\frac{\partial \varsigma'}{\partial t} = -\bar{u}\frac{\partial \varsigma'}{\partial x} - \bar{v}\frac{\partial \varsigma'}{\partial y} - u'\frac{\partial \bar{\zeta}}{\partial x} - v'\frac{\partial(\bar{\zeta}+f)}{\partial y} + (\bar{\zeta}+f)\frac{\partial \omega'}{\partial p} - K_v\zeta' - \gamma\nabla^2\zeta' + F_{eddy} \qquad (2).$$

where ς is the relative vorticity, primes denote perturbation quantities, and overbars denote basic-state quantities. In this equation, $(\bar{\zeta}+f)\frac{\partial \omega'}{\partial p}$ is the stretching term. Calculations suggest that this term, along with the linear damping and diffusion terms, is unimportant for the vorticity budget in comparison with the first four terms on the right side. Area means, over the north and south lobes of the response, of these four terms were calculated, and the results are summarized in Table 1. For the negative vorticity of the northern lobe, the most important vorticity source is the term $-u'\frac{\partial \bar{\zeta}}{\partial x}$, i.e., the zonal advection of background vorticity by perturbation wind. The northward lobe can, therefore, be considered the local response to the zonal advection of basic state vorticity due to the cyclonic circulation induced by the eddy forcing. This confirms the importance of the zonal gradient of background vorticity in forming such a dipolar response.

Additional LBM experiments are performed using a zonal symmetric basic flow (lacking a zonal gradient of basic-state vorticity). The results (not shown) suggest no south-north dipole response regardless of the latitude of the forcing. Thus, the dipolar linear response to the transient forcing locating at the jet exit can be indeed attributed to the substantial zonal gradient of background vorticity.

4.3 Dynamics of nonlinear response

As discussed in PRL03, the sign-asymmetry in the SST-induced response may result from various nonlinear interactions involving the heating- and eddy-induced anomalous flows. This issue is investigated by performing experiments with the barotropic model (BVM) driven by the heating-induced transient vorticity forcing shown in Fig. 4c. We seek to determine the contribution of the nonlinear self-interaction of the transient-eddy-induced quasi-stationary perturbation to the sign-nonlinearity by considering the sensitivity to the sign and the strength of this transient-eddy forcing. To give prominence to primary signals, the tripolar forcing components shaded in Fig. 4c are used for the BVM experiments. The strength of the vorticity forcing is varied by multiplicative factor between 1 to 10. Figure 9 shows the BVM response for two strengths of forcings. For the original heating-induced forcing, the weaker one, the response is symmetric about the sign of the forcing. It projects on the NAO, though not as strongly as the linear baroclinic response shown in Fig. 5a. For the stronger forcing, with the strength multiplied by a factor of 8, nonlinearity is more evident, and the sign asymmetry resembles that obtained from the AGCM results. The response to the positive forcing is a meridional dipole projecting on the NAO, while the response to the sign-reversed forcing exhibits a stronger wave train component. The magnitude of the nonlinear component is about one-third as big as the linear, also consistent with that in the AGCM (compare

Fig. 9c and 2d). Furthermore, when the individual components of the transient-eddy forcing component are used to force the BVM, the results reveal that such a nonlinearity is primarily induced by the middle component in the jet exit.

The BVM results suggest that nonlinear barotropic vorticity dynamics may contribute to the sign-nonlinearity of the response in the AGCM. This nonlinearity emerges, however, only when the strength of the forcing is significantly enhanced from that in the AGCM. On one hand, this may be due to the limitation of barotropic dynamics in describing the interaction between the synoptic baroclinic eddy and basic flow, albeit eddies are quasi-barotropic in their decaying stage. On the other hand, other nonlinear interactions, like those between, or in-between, the heating-induced and transient-induced perturbations discussed in PRL03, may also be important in generating the sign-nonlinearity in the AGCM response.

Because the mechanism for nonlinearity in the BVM, the self-advection of the response to anomalous forcing, does not depend on the SST anomaly, such nonlinearity should also be present in the intrinsic variability of the AGCM. Whether this is true in the present AGCM is addressed by comparing the composite 500-hPa height anomalies in the AGCM control runs when the transient forcing in the exit of the Atlantic jet is strongly negative or positive. Monthly 300-hPa streamfunction tendencies due to transient eddies at (40^{o}W, 40^{o}N) with values, normalized by the standard deviations for that calendar month, greater than 0.65 (less than -0.65) comprise the anomalous transient-eddy-forcing cases. Forty negative (76 positive) anomalous months are found among the 300 February-April months in the 100 control runs. Figure 10 shows the composite 500-hPa heights. These composites largely resemble the BVM response to idealized negative/positive transient forcing (cp. Fig. 10 with Fig. 9a-c) and also the AGCM response to the positive/negative SSTA (compare Fig. 10 with Fig. 1a, e, 2d). The magnitude of the nonlinear component is also

about one-third of the linear. This suggests that the nonlinear response to the SSTA may in part be attributed to the advection of the perturbation response by the perturbation flow induced by a positive or negative vorticity anomaly in the jet exit, which is, in turn, a response to eddy forcing. In Fig. 10a, the cyclonic flow resulting from positive vorticity (negative streamfunction) forcing distorts a classic Rossby wave-train response in the sense of sweeping the first downstream positive streamfunction anomaly to the north of the forcing region, yielding a meridional dipole. Conversely, in Fig. 10b the anticyclonic flow resulting from negative vorticity (positive streamfunction) forcing carries the first downstream negative streamfunction anomaly to the east of the forcing region, and the resulting downstream wavetrain propagates into the tropics.

5. Summary and discussions

Previous model experiments, in which the NCEP AGCM for seasonal prediction was forced by a tropical Atlantic SST anomaly, yielded a response that projected strongly on the North Atlantic Oscillation. The characteristic meridional dipole of the NAO, however, was a response to the positive SST anomaly, which produced a negative NAO. On the other hand, a negative SST anomaly produced a positive geopotential anomaly in the southern center of action of the NAO, but little response in the northern center of action. Instead, the downstream response was a stationary Rossby wavetrain propagating to the east. The response to a tropical SSTA could thus be separated into a notionally linear response, computed as the difference between the responses to positive and negative SSTA, and a notionally nonlinear response, computed from the average of the responses to the positive and negative SSTA. Here we explore the dynamics of these linear and nonlinear responses.

Using a linear baroclinic model, we find, consistent with results for midlatitude SSTA and for SSTA associated with ENSO, that the extratropical responses are dominated by the responses to transient-eddy forcing. In particular, the NAO response results from transient-eddy forcing centered in the jet exit. Experiments in which an idealized forcing is applied at many different locations indicate that this is a preferred location for inducing the NAO meridional dipole. The induction of a meridional dipole from forcing in this location depends on the structure of the basic state flow, namely the presence of a significant zonal component in the gradient of absolute vorticity. Results from a statistical stormtrack model indicate that eddy forcing in this location results when the basic state is perturbed by the linear response to tropical heating. Thus, these results support the eddy-feedback mechanism proposed by Peng and Whitaker (1999) to explain the atmospheric response to an SSTA in the extratropical North Pacific.

A possible dynamical origin of the nonlinear component of the response is explored by forcing a nonlinear barotropic model with an initial heating-induced transient-eddy forcing. Results from this model suggest that the asymmetry in the response to positive and negative SST anomalies may, in part, result from the self-advection of the perturbation induced by transient-eddy forcing, especially, once again, when the forcing is centered in the jet exit. This appears to be consistent with the nonlinearity in the response to the intrinsic model variability forced by internally generated variability in the transient eddy forcing in this key region. We note, however, that the sign-nonlinearity in BVM is significant only when the transient forcing is substantially enhanced, and suspect that other nonlinear mechanisms may also be at work in the asymmetric GCM response, such as those discussed in PRL03.

The mechanisms that produce the linear and nonlinear responses to a tropical Atlantic SST considered here can be summarized as follows: first, the tropical Atlantic SSTA induces anomalous

heating over the SSTA. This heating is nearly symmetric with respect to the sign of SSTA. The heating anomaly induces a Rossby wave train that propagates from the tropics and across the North Atlantic to Europe. This anomalous flow perturbs the storm track, and results in anomalous transient-eddy forcing that is strongest in the jet exit. This anomalous transient-eddy forcing acts linearly on the time-mean flow to induce an NAO-like meridional dipole. When the nonlinearity of this response is included, the symmetry of the linear dipole is broken by the self-advection of the perturbation response. The dynamics of both the linear and nonlinear responses are general, in that they should apply to other perturbation that induces flow anomalies in the extratropical storm tracks.

One may question whether this sequence of mechanisms can actually operate within the course of a winter season. In the atmosphere, it takes about one week to establish a steady heating anomaly for a fixed tropical SSTA. As discussed in Jin and Hoskins (1995), the extratropical direct linear response to a tropical forcing develops fully in about two weeks. The time scale for establishing the tropical and middle-latitude patterns is about one week and that for the higher-latitude pattern is less than one additional week. Therefore, it takes about one month or slightly longer to establish a stable extratropical response to a tropical SSTA. Since the dynamics for sign-nonlinearity are associated with the self-interaction of quasi-stationary perturbations induced by heating or transient forcing, the nonlinear response should develop primarily within the last two weeks of this period. For a strong tropical Atlantic SSTA, there is sufficient time in a winter season for a fully-developed sign-asymmetric circulation anomaly to develop. The above processes include only the interactions between synoptic-scale eddies and quasi-stationary time-mean flow. The role of eddies with timescales greater than the synoptic but less than one season, and how such eddies interact with synoptic eddies and the time-mean flow, are not addressed and need to be studied.

Is a similar sign-asymmetry present in the observed responses to tropical Atlantic SSTA? In view of the lead-lag relationship between the fall SSTA pattern and the winter NAO in CF02, observational composite analyses are performed for the months in October-December when the tropical Atlantic SSTA has a positive or negative projection on the tropical component of the pan-Atlantic SST pattern. Monthly mean geopotential heights from the NCEP-NCAR (National Center for Atmospheric Research) reanalysis (Kalnay et al. 1996) and the Global Ice and Sea Surface Temperature dataset (GISST) (Rayner et al. 1996) in 1948-1999 are used. As in CF02, a filter is applied to these two datasets to remove the trends and the low frequencies (interannual to decadal time scales). Because there are few months when the tropical Atlantic SSTA reaches 1.2^{o}C, the amplitude of the SSTA used in the AGCM (Fig. 1d), the results are not readily comparable to the AGCM simulations. Since the sign-asymmetry is negligible for a weak forcing but increases along with the forcing strength, the composite circulation anomalies for the positive and negative SSTA months with varying strengths may reveal sign-asymmetry. From Fig. 11, for the SSTA amplitude of about 0.6^{o}C (Fig. 11a and b), the composite 500-hPa height anomaly exhibits a sign-asymmetry to some extent, which is seen from the differing orientation of the dipole axis (Fig. 11c and d). For a weaker SSTA, the composite anomaly projects on the NAO, more resembles the linear response in the AGCM (cp. Fig. 11e and f with Fig. 2a), and is largely linear about the SSTA sign. Thus, there is some evidence that the sign-asymmetry exists in observations when the tropical Atlantic SSTA is sufficiently strong.

Acknowledgements.

The significant contributions by Shiling Peng to attributing the origin of the linear response component are gratefully acknowledged. SL is grateful to GFDL's Amy Longenhorst, William Cooke, and Peter Phillips for their assistance in configuring the barotropic vorticity equation

model, and to Jeffrey Whitaker for providing the linear baroclinic model. We are thankful to the editor, David M. Straus, and the four anonymous reviewers for their helpful comments. This study is supported in part by the NOAA CLIVAR Atlantic program.

References

Barnett, T.P., 1985: Variations in near-global sea level pressure. *J. Atmos. Sci*. **42**, 478–501.

Branstator, G., 1992: The maintenance of low-frequency atmospheric anomalies. *J. Atmos. Sci.*, **49**, 1924-1945.

Branstator, G., 2002: Circumglobal teleconnections, the jetstream waveguide, and the North Atlantic Oscillation. *J. Climate*, **15**, 1893-1910.

Czaja, A., and C. Frankignoul, 2002: Observed impact of Atlantic SST anomalies on the North Atlantic Oscillation. *J. Climate*, **15**(6), 606-623.

Deser, C., G. Magnusdottir, R. Saravanan, and A. Phillips, 2004: The effects of North Atlantic SST and sea-ice anomalies on the winter circulation in CCM3, Part II: Direct and indirect components of the response. *J. Climate,* **17**, 877-889.

Drevillon, M., C. Cassou, and L. Terray, 2003: Model study of the North Atlantic regional atmospheric response to autumn tropical Atlantic seas-surface-temperature anomalies. *Q. J. R. Meteorol. Soc.*, **129**, 2591-1611.

Feldstein. S. B., 2000: The timescale, power spectra, and climate noise properties of teleconnection patterns. *J. Climate*, **13**, 4430–4440.

Held, I. M., and P. J. Phillips, 1987: Linear and nonlinear barotropic decay on the sphere. *J. Atmos. Sci*., **44**, 200-207.

Hoerling, M. P., A. Kumar, and M. Zhong, 1997: El Nino, La Nina, and the nonlinearity of their teleconnections. *J. Climate*, **10**, 1769-1786.

Hoerling, M. P., J. Hurrell, and T. Xu, 2001: Tropical origins for North Atlantic climate change. *Science*, **292**, 90-92.

Hoerling, M. P., and A. Kumar, 2002: Atmospheric response patterns associated with tropical forcing. *J. Climate*, **15**, 2184-2203.

Horel, J. D., and J. M. Wallace, 1981: Planetary scale atmospheric phenomena associated with the Southern Oscillation. *Mon. Wea. Rev.,* **109**, 813–829.

Hoskins, B. J., and D. J. Karoly, 1981: The steady linear response of a spherical atmosphere to thermal and orographic forcing. *J. Atmos. Sci.,* **38**, 1179–1196.

Kalney, E., and coauthors, 1996: The NCEP/NCAR 40-Year Reanalysis Project. *Bull. Amer. Meteor. Soc*., **77**, 437-471.

Kanamitsu, M., and co-authors, 2002: NCEP dynamical seasonal forecast system 2000. *Bull. Amer. Metero. Soc.*, 83, 1019-1037.

Kushnir, Y., and N. C. Lau, 1992: The general circulation model response to a North Pacific SST anomaly: dependent on timescale and pattern polarity. *J. Climate*, **5**, 271-283.

Kushnir, Y., W. A. Robinson, I. Blade, N. M. J. Hall, S. Peng and R. Sutton, 2002: Atmospheric GCM response to extratropical SST anomalies: Synthesis and evaluation. *J. Climate*, **15**(16), 2233-2256.

Lau, N.-C., and M. J. Nath, 1991: Variability of the baroclinic and barotropic transient eddy forcing associated with monthly changes in the midlatitude storm tracks. *J. Atmos. Sci*., **48**, 2589-2613.

Li, S., 2004: Impact of Northwest Atlantic SST anomalies on the circulation over the Ural Mountains during early winter. *J. Meteor. Soc. Japan*, **82**(4), 971-988.

Li, S.**,** M. P. Hoerling, S. Peng, and K. M. Weickmann, 2006a: The annular response to tropical Pacific SST forcing. *J. Climate,* **19**(9), 1802–1819.

Li, S., M. P. Hoerling, and S. Peng, 2006b: Coupled ocean-atmosphere response to Indian Ocean warmth. *Geophy. Res. Lett.* **33**(7), L07713,10.1029/2005GL025558.

Lin, H., and J. Derome, 1995: On the thermal interaction between the synoptic-scale eddies and the intra-seasonal fluctuations in the atmosphere. *Atmos.–Ocean,* **33**, 81–107.

Lin, H., and J. Derome 2004: Nonlinearity of the extratropical response to tropical forcing. *J. Climate*, **17**, 2597-2608.

Jin, F., and B. J. Hoskins, 1995: The direct response to tropical heating in a baroclinic atmosphere. *J. Atmos. Sci*., **52**, 307-319.

Magnusdottir, G., C. Deser, and R. Saravanan, 2004: The effects of North Atlantic SST and sea-ice anomalies on the winter circulation in CCM3, Part I: Main features and storm-track characteristics of the response. *J. Climate*, **17**, 857-876.

Peng, S., and J. S. Whitaker, 1999: Mechanism determining the atmospheric response to midlatitude SST anomalies. *J. Climate*, **12**, 1393-1408.

--------, W. A. Robinson, and S. Li, 2002: North Atlantic SST forcing of the NAO and relationship with intrinsic hemispheric variability. *Geophys. Res. Lett*., **29**, 1276, doi:10.1029/2001GL 014043

--------, W. A. Robinson, and S. Li, 2003: Mechanisms for the NAO responses to the North Atlantic SST tripole. *J. Climate*, **16**(12), 1987-2004.

--------, --------, --------**,** and M.P. Hoerling, 2005: Tropical Atlantic SST forcing of coupled North Atlantic seasonal responses. *J. Climate,* **18**, 480-496.

Pitcher, E. J., M. L. Blackman, G. T. gates, and S. Munoz, 1988: The effect of North Pacific sea surface temperature anomalies on the January climate of a general circulation model. *J. Atmos. Sci*., **45**, 171-188.

Rayner, N. A., E. B. Horton, D. E. Parker, C. K. Folland, and R. B. Hackett, Version 2.2 of the global sea surface temperature data set, 1903-1994, *Climate Research Technical Note 74*, Hadley Center for Climate Prediction and Research, UK Meteorological Office, 1996.

Robinson, W. A., S. Li, and S. Peng, 2003: Dynamical nonlinearity in the atmospheric response to Atlantic sea surface temperature anomalies. *Geophys. Res. Lett*., **30**(20), 2038,doi:10.1029/2003GL018416.

Saravanan, R., 1998: Atmospheric low frequency variability and its relationship to midlatitude SST variability: Studies using NCAR Climate System Model. *J. Climate*, **11**, 1386-1404.

Simmons, A. J., 1982: The forcing of stationary wave motion by tropical diabatic heating. *Quart. J. Roy. Meteor. Soc.,* **108**, 503–534.

Sutton, R. T., W. A. Norton, and S. P. Jewson, 2000: The North Atlantic Oscillation-what role for the ocean? *Atmos. Sci. Lett*., **1**, 89-100.

Ting, M., and N.-C. Lau, 1993: A diagnostic and modeling study of the monthly mean wintertime anomalies appearing in a 100-year GCM experiment. *J. Atmos. Sci.,* **50**, 2845-2867.

van Loon, H., and J. C. Rogers, 1981: The Southern Oscillation. Part II: Associations with changes in the middle troposphere in the northern winter. *Mon. Wea. Rev.,* **109**, 1163–1168.

Table 1. Area-mean perturbation vorticity tendency diagnosed from the LBM dipolar response in Fig. 8a when the forcing is prescribed centering at (40°W, 40°N). Unit: 10^{-11} S^{-2}.

	$-\bar{u}\frac{\partial \varsigma'}{\partial x}$	$-\bar{v}\frac{\partial \varsigma'}{\partial y}$	$-u'\frac{\partial \bar{\varsigma}}{\partial x}$	$-v'\frac{\partial(\bar{\zeta}+f)}{\partial y}$
Northern Lobe (40W-0, 50-70N)	-0.24	0.34	-0.64	0.04
Southern Lobe (60-10W, 30-50N)	-1.07	1.38	-0.76	0.41

Figure Captions

Fig. 1 February-April mean response of geopotential heights at 500-hPa (a, e) and in the cross-section along 45°N (b, f), 300-hPa transient vorticity forcing expressed as streamfunction tendency (c, g), and tropical precipitation (d, h). (a, b, c, d) is for the positive SSTA, and (e, f, g, h) is for the sign-reversed SSTA. Unit: gpm in (a, b, e, f), $m^2 s^{-2}$ in (c, g), and mm day^{-1} in (d, h). Shading indicates significance at the 95% level estimated by Student's *t* test, except for d) where represents the SSTA used for the experiments with contours from 0.3 (lightest) to 1.2°C (heaviest).

Fig. 2 Symmetric (a, b, c) and antisymmetric (d, e, f) component of 500-hPa height response and 300-hPa transient vorticity forcing. (a, d) height response in the AGCM, (b, e) combined height response in the LBM to the anomalous transient eddy forcing and to the anomalous diabatic heating. (c, f) transient vorticity forcing. Unit: gpm in (a, b, d, e), and $m^2 s^{-2}$ in (c, f). Shading indicates significant at the 95% level.

Fig. 3 As Fig. 2b and e, 500-hPa height response in the LBM to the anomalous transient forcing (a, c), and to the anomalous diabatic heating (b, d), respectively. Unit: gpm.

Fig.4 a) In-depth averaged heating rate of an idealized heating with the maximum at 600-hPa. Unit: K day^{-1}.

b) LBM 300-hPa geopotential height response to the idealized heating in a). Unit: gpm.

c) STM-predicted 300-hPa transient eddy forcing response to the anomalous flow in (b). Unit: $m^2 s^{-2}$. The components shaded and marked with "S", "M" and "N" have their individual influences compared in Fig. 5.

d) LBM 300-hPa geopotential height response to the anomalous transient forcing in (c). Unit: gpm.

Fig. 5 As Fig. 4d, but to the combined or individual anomalous transient forcing components shaded in Fig. 4c. (a) to the combined, and (b-d) to the northern "N", middle "M" and southern "S" component, individually. Unit: gpm.

Fig. 6 Vertical profile (a) and in-depth mean (b) of an idealized transient forcing, with the maximum location shifted around the exit sector of the jet (solid circle dots in (c)). The contour in (c) indicates the February-April mean 300-hPa zonal wind in the control runs. Unit: $m^2 s^{-2}$ in (a, b) and $m s^{-1}$ in (c).

Fig. 7 Examples of LBM 500-hPa height response to the idealized transient forcing with various locations in Fig. 6. Unit: gpm.

Fig. 8 a) Combined plot of the LBM 500-hPa height response (thick solid for positive value and dotted line for negative value. Only displayed are the contours -15, -10, 10, 15, 20. Unit: gpm. Also see Fig. 7e), the transient forcing (shading, also see Fig. 6c), and the 300-hPa background absolute vorticity (thin dashed line, contour interval: $1.0\ 10^{-5}\ S^{-1}$) when the forcing is prescribed centering at (40^oW, 40^oN).

b) Schematic diagram for the dipolar response to a transient forcing around the jet exit sector. Thick solid line: background absolute vorticity. Thin solid line: geopotential height response with "L" to represent a low, and "H" a high. Elliptical shading marked by "F" represents the transient eddy forcing.

Fig. 9 Comparison of BVM geopotentional height response to a transient forcing with different strength. The forcing is extracted from the initial heating-induced transient forcing in Fig. 4c. (a) for an amplified forcing by a factor 8. (b), as (a), but with the forcing sign reversed. (c) antisymmetric component in (a) and (b) estimated by one half of their sum. (d-f), as (a-c), but for the original extracted forcing. Unit: gpm. The BVM is applied at 300-hPa.

Fig.10 Composite of 500-hPa geopotential height anomaly for the months in February-April when the transient forcing anomaly around the Atlantic jet exit (40^{o}W, 40^{o}N) is strongly positive (a) and negative (b) in the control runs. (c) the antisymmetric component between (a) and (b). Unit: gpm. Shading is significant at the level of 95%.

Fig. 11 Composite SSTA (a, b) (unit: ^{o}C) and 500-hPa geopotential heights (c, d) (unit: m) for the 53 positive and 49 negative SSTA months within October to December through 1948-1999 when the normalized SSTA projection coefficients on the tropical component of the Pan-Atlantic pattern are greater than 0.5 or less than -0.5. (e, f), as (c, d), but for the 63 positive and 61 negative SSTA months when the normalized projection coefficients are greater than 0.3 or less than -0.3. The thick solid line in (c-f) is the axis line of the height dipole for comparison. Shading in (c-f) is significant at the level of 90%.

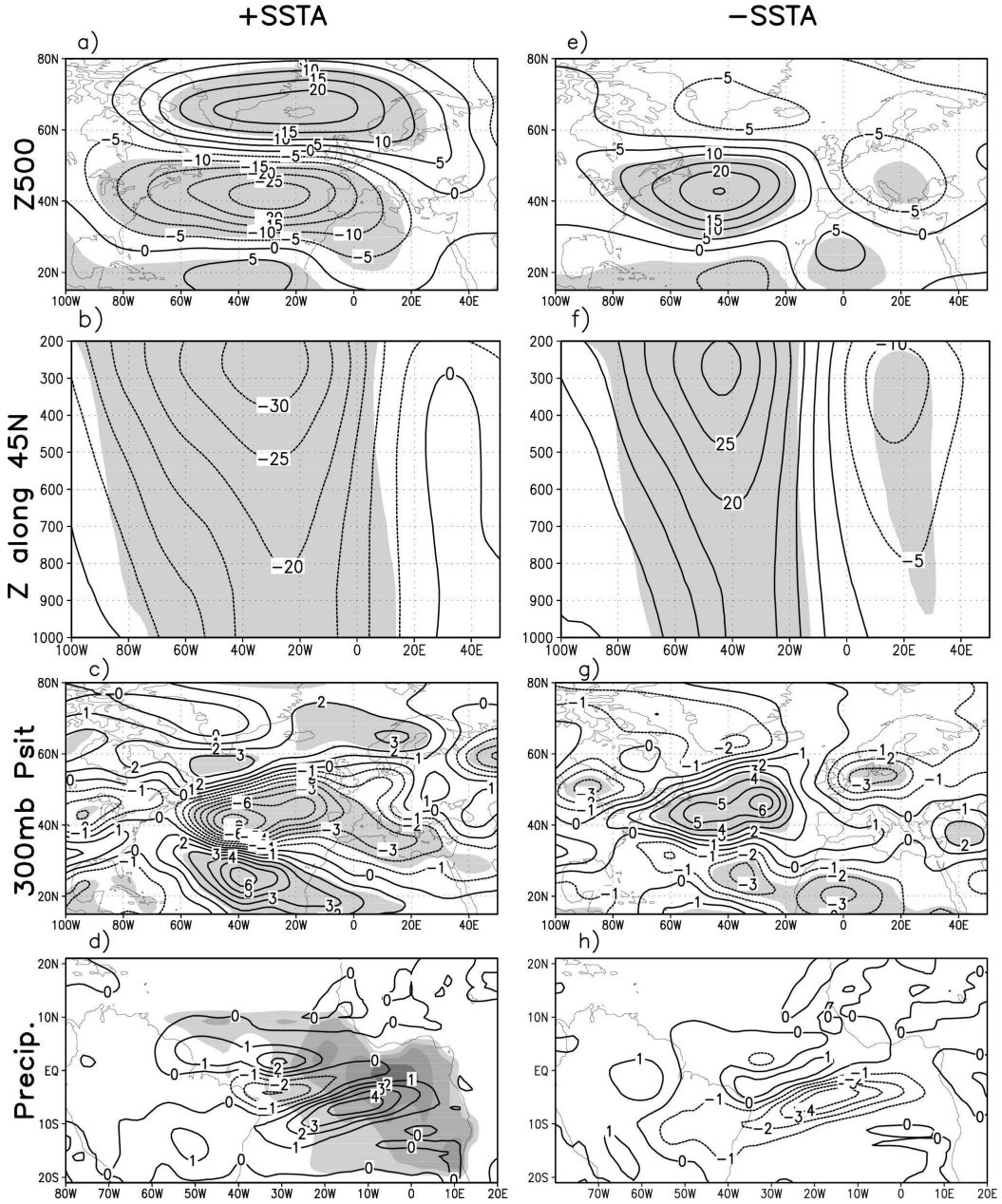

Fig. 1 February-April mean response of geopotential heights at 500-hPa (a, e) and in the cross-section along 45°N (b, f), 300-hPa transient vorticity forcing expressed as streamfunction tendency (c, g), and tropical precipitation (d, h). (a, b, c, d) is for the positive SSTA, and (e, f, g, h) is for the sign-reversed SSTA. Unit: gpm in (a, b, e, f), $m^2 s^{-2}$ in (c, g), and mm day^{-1} in (d, h). Shading indicates significance at the 95% level estimated by Student's *t* test, except for d) where represents the SSTA used for the experiments with contours from 0.3 (lightest) to 1.2°C (heaviest).

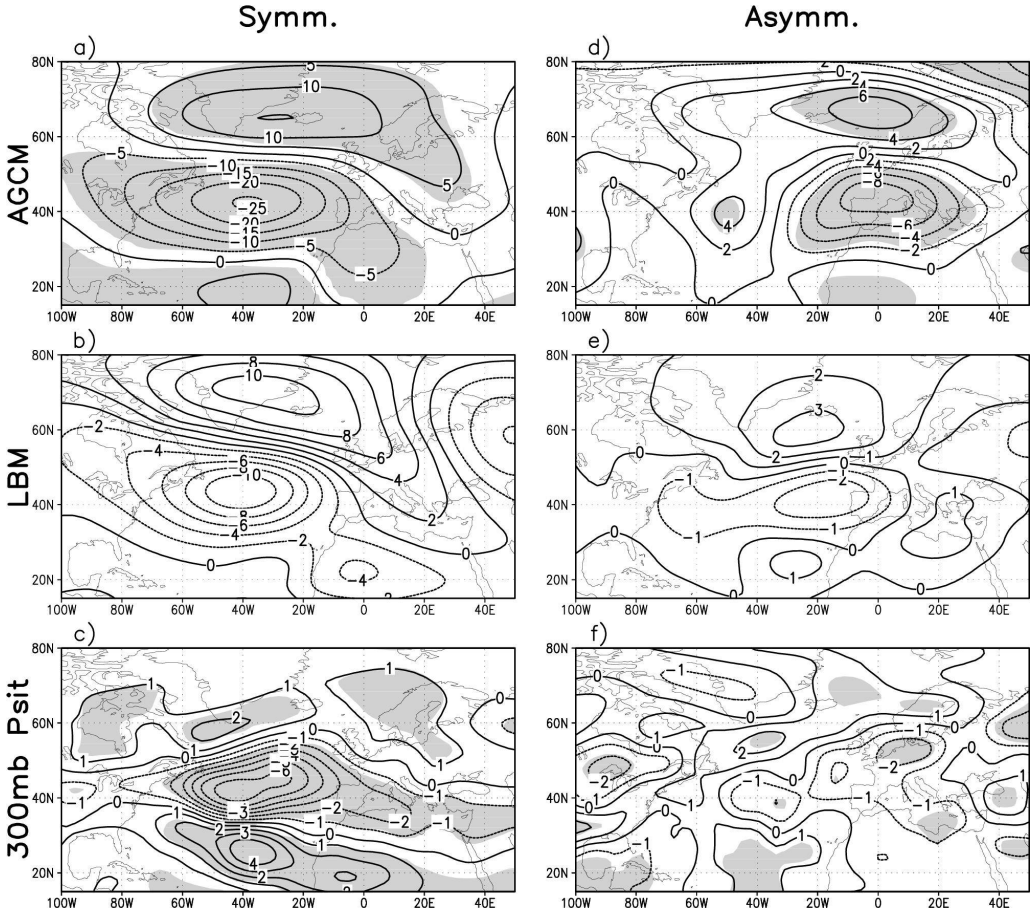

Fig. 2 Symmetric (a, b, c) and antisymmetric (d, e, f) component of 500-hPa height response and 300-hPa transient vorticity forcing. (a, d) height response in the AGCM, (b, e) combined height response in the LBM to the anomalous transient eddy forcing and to the anomalous diabatic heating. (c, f) transient vorticity forcing. Unit: gpm in (a, b, d, e), and $m^2 s^{-2}$ in (c, f). Shading indicates significant at the 95% level.

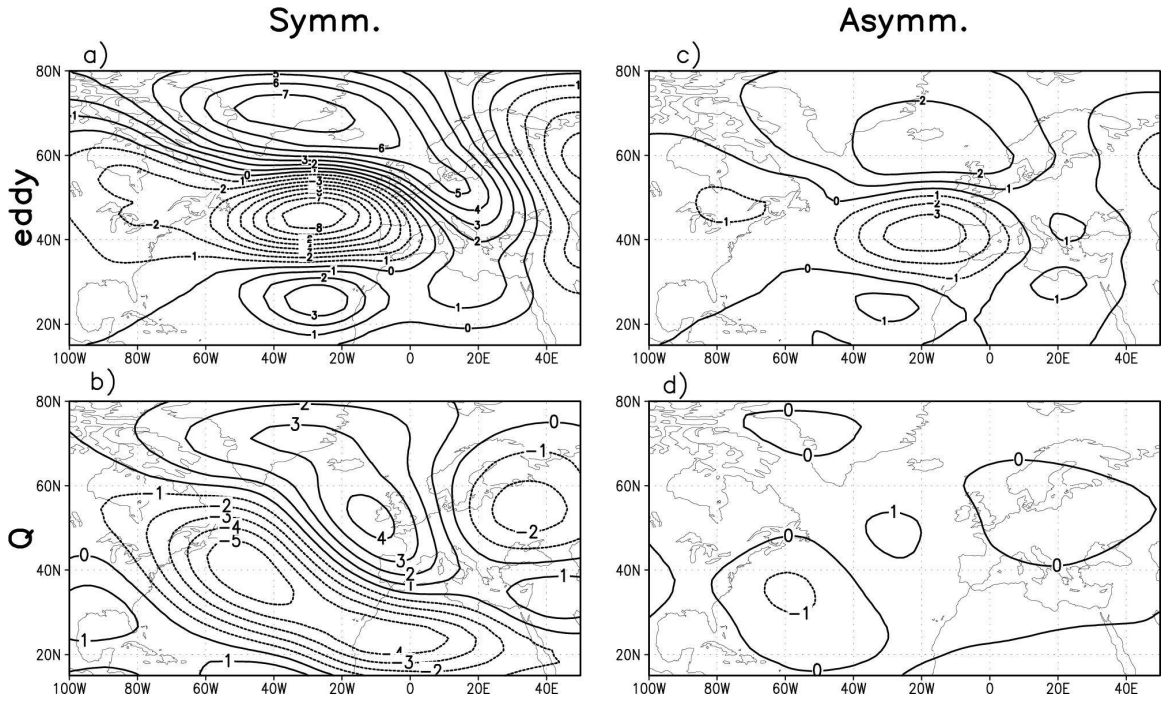

Fig. 3 As Fig. 2b and e, 500-hPa height response in the LBM to the anomalous transient forcing (a, c), and to the anomalous diabatic heating (b, d), respectively. Unit: gpm.

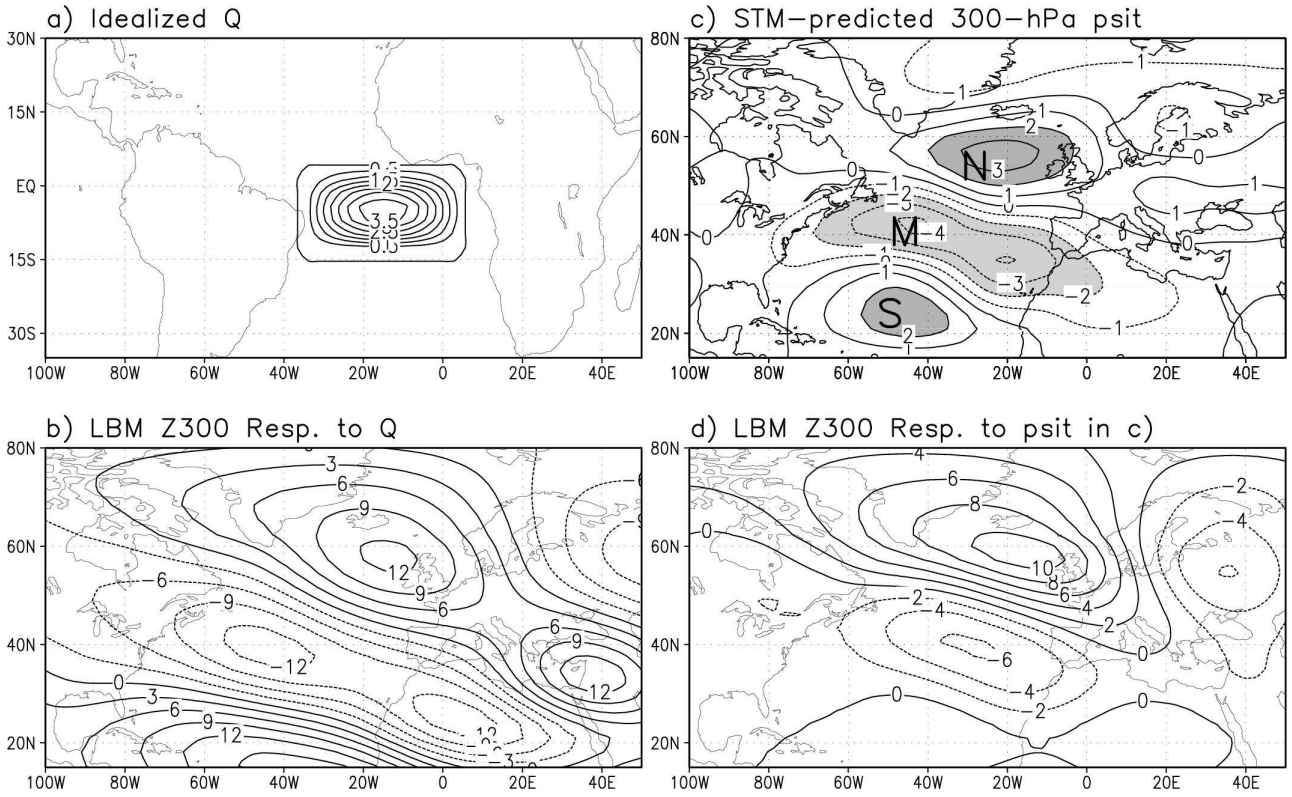

Fig.4 a) In-depth averaged heating rate of an idealized heating with the maximum at 600-hPa. Unit: K day^{-1}.

b) LBM 300-hPa geopotential height response to the idealized heating in a). Unit: gpm.

c) STM-predicted 300-hPa transient eddy forcing response to the anomalous flow in (b). Unit: m^2s^{-2}. The components shaded and marked with "S", "M" and "N" have their individual influences compared in Fig. 5.

d) LBM 300-hPa geopotential height response to the anomalous transient forcing in (c). Unit: gpm.

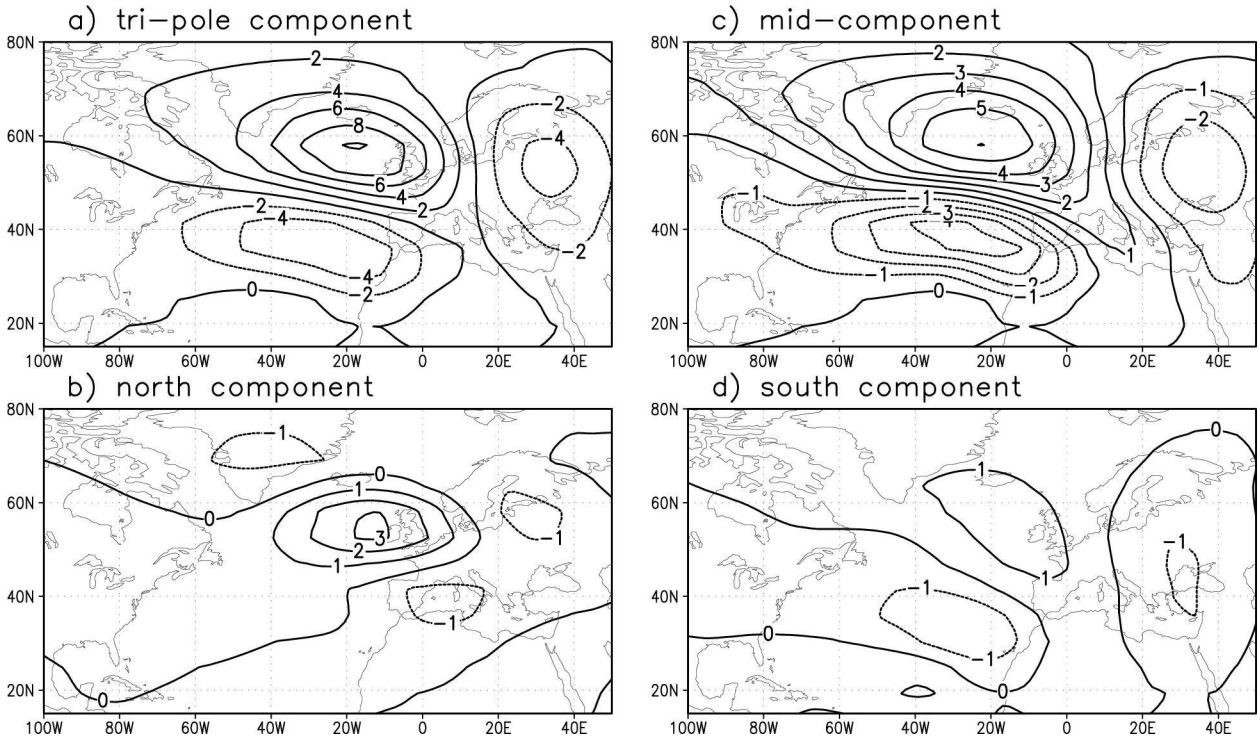

Fig. 5 As Fig. 4d, but to the combined or individual anomalous transient forcing components shaded in Fig. 4c. (a) to the combined, and (b-d) to the northern "N", middle "M" and southern "S" component, individually. Unit: gpm.

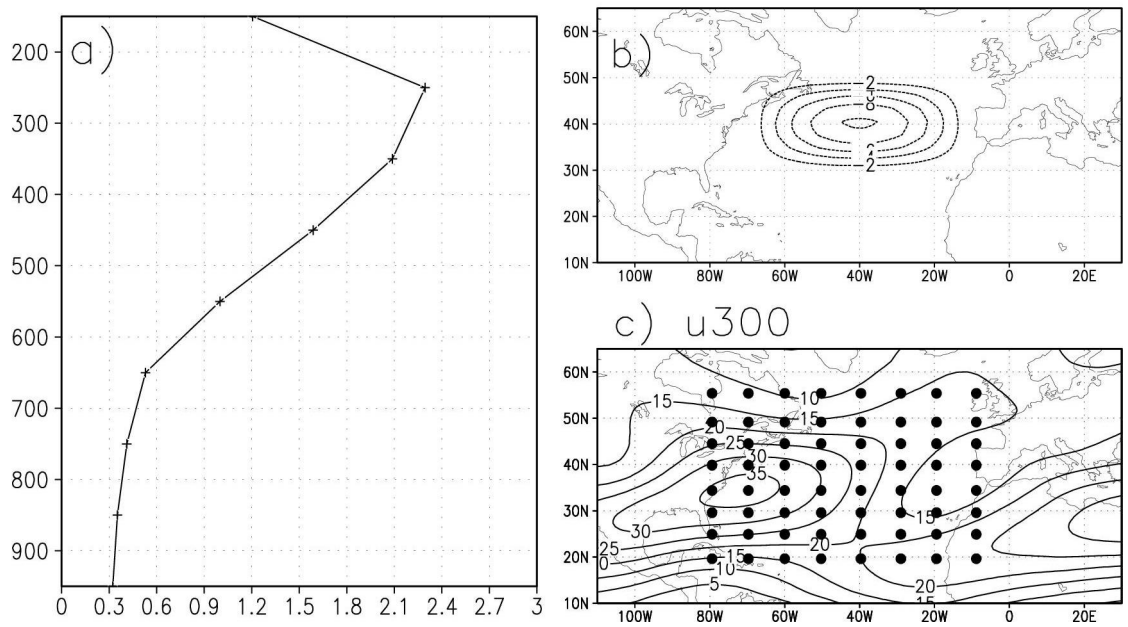

Fig. 6 Vertical profile (a) and in-depth mean (b) of an idealized transient forcing, with the maximum location shifted around the exit sector of the jet (solid circle dots in (c)). The contour in (c) indicates the February-April mean 300-hPa zonal wind in the control runs. Unit: $m^2 s^{-2}$ in (a, b), and $m s^{-1}$ in (c).

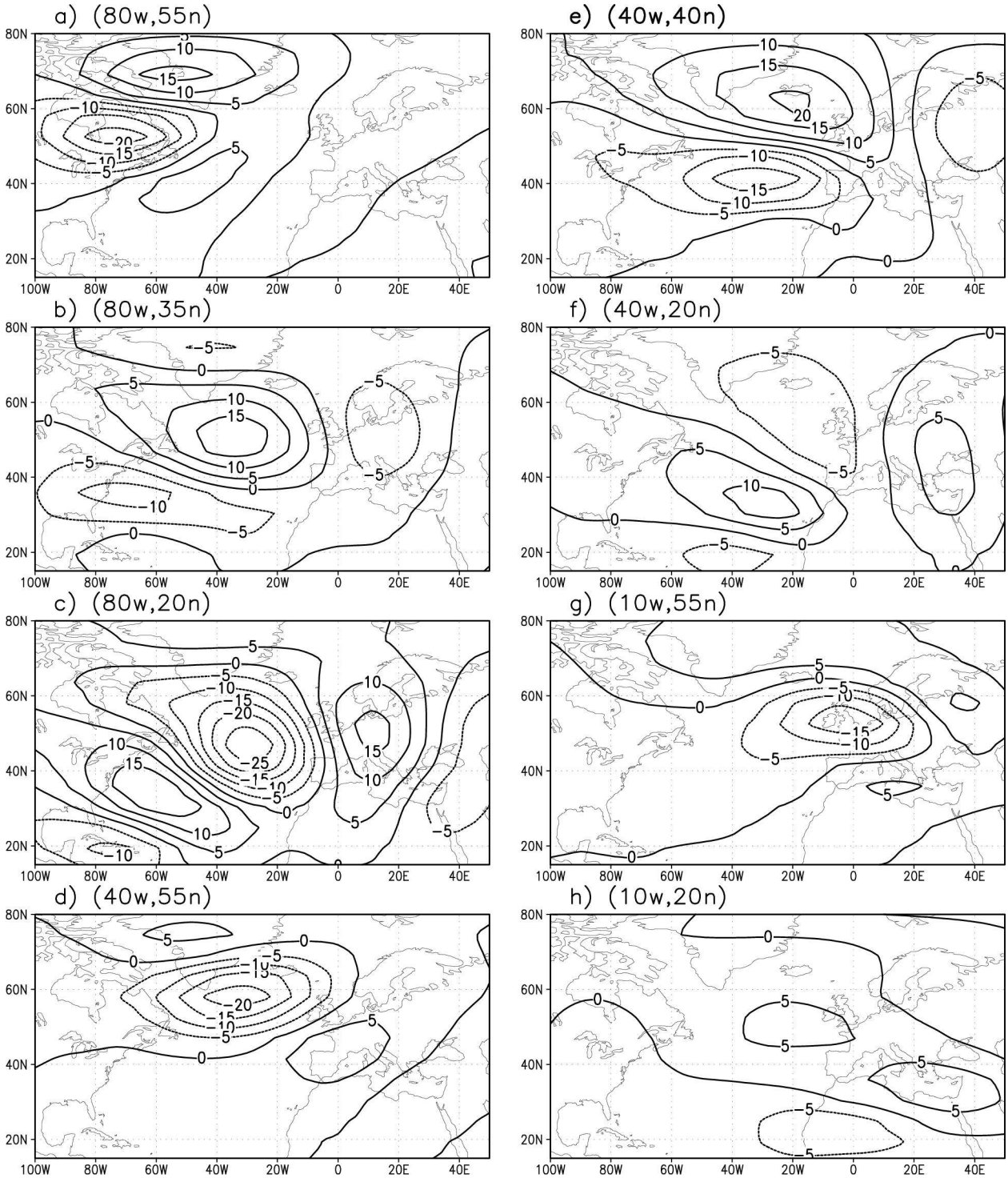

Fig. 7 Examples of LBM 500-hPa height response to the idealized transient forcing with various locations in Fig. 6. Unit: gpm.

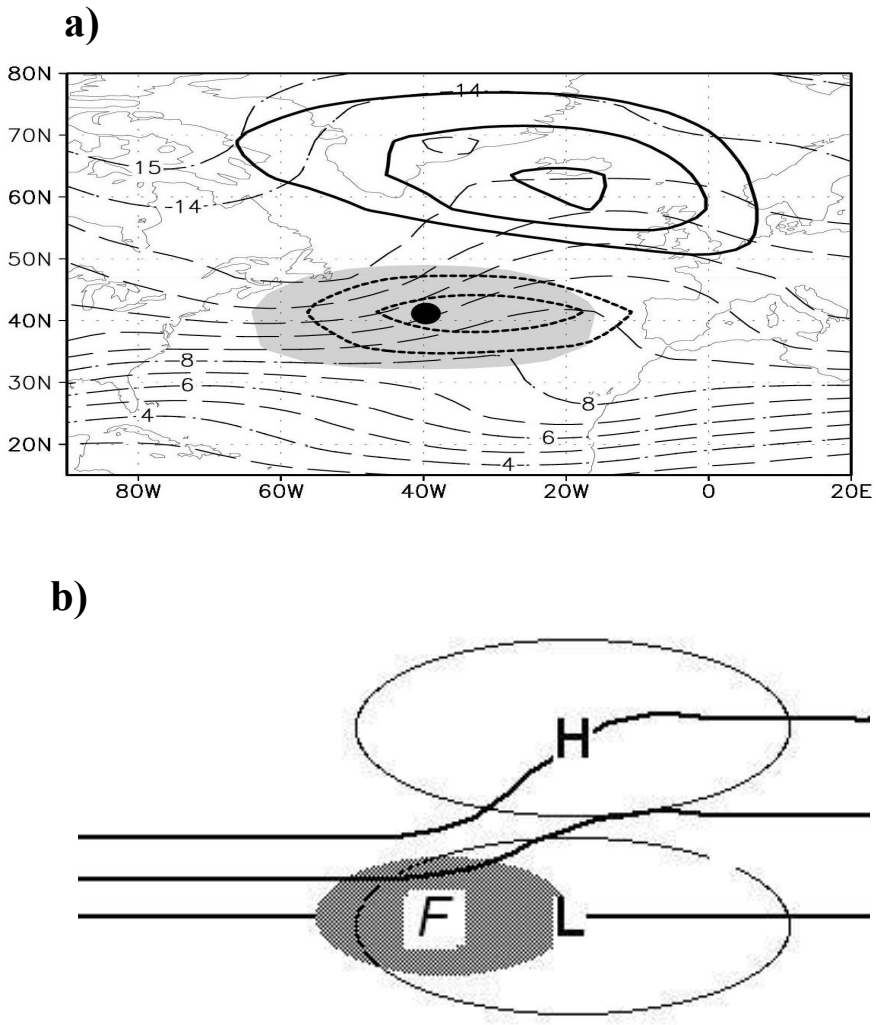

Fig. 8 a) Combined plot of the LBM 500-hPa height response (thick solid for positive value and dotted line for negative value. Only displayed are the contours -15, -10, 10, 15, 20. Unit: gpm. Also see Fig. 7e), the transient forcing (shading, also see Fig. 6c), and the 300-hPa background absolute vorticity (thin dashed line, contour interval: 1.0 10^{-5} S^{-1}) when the forcing is prescribed centering at (40°W, 40°N).

b) Schematic diagram for the dipolar response to a transient forcing around the jet exit sector. Thick solid line: background absolute vorticity. Thin solid line: geopotential height response with "L" to represent a low, and "H" a high. Elliptical shading marked by "F" represents the transient eddy forcing.

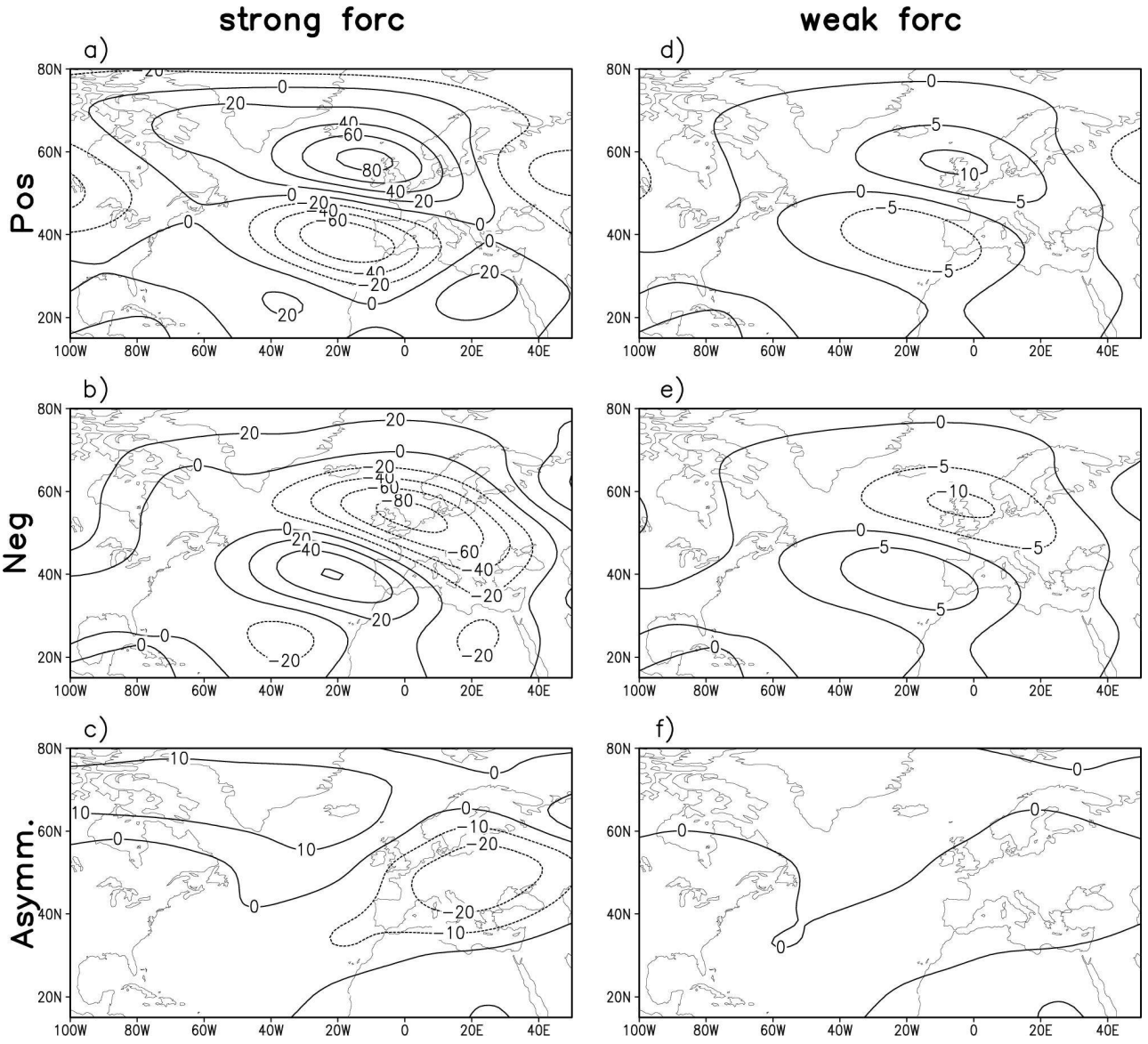

Fig. 9 Comparison of BVM geopotentional height response to a transient forcing with different strength. The forcing is extracted from the initial heating-induced transient forcing in Fig. 4c. (a) for an amplified forcing by a factor 8. (b), as (a), but with the forcing sign reversed. (c) antisymmetric component in (a) and (b) estimated by one half of their sum. (d-f), as (a-c), but for the original extracted forcing. Unit: gpm. The BVM is applied at 300-hPa.

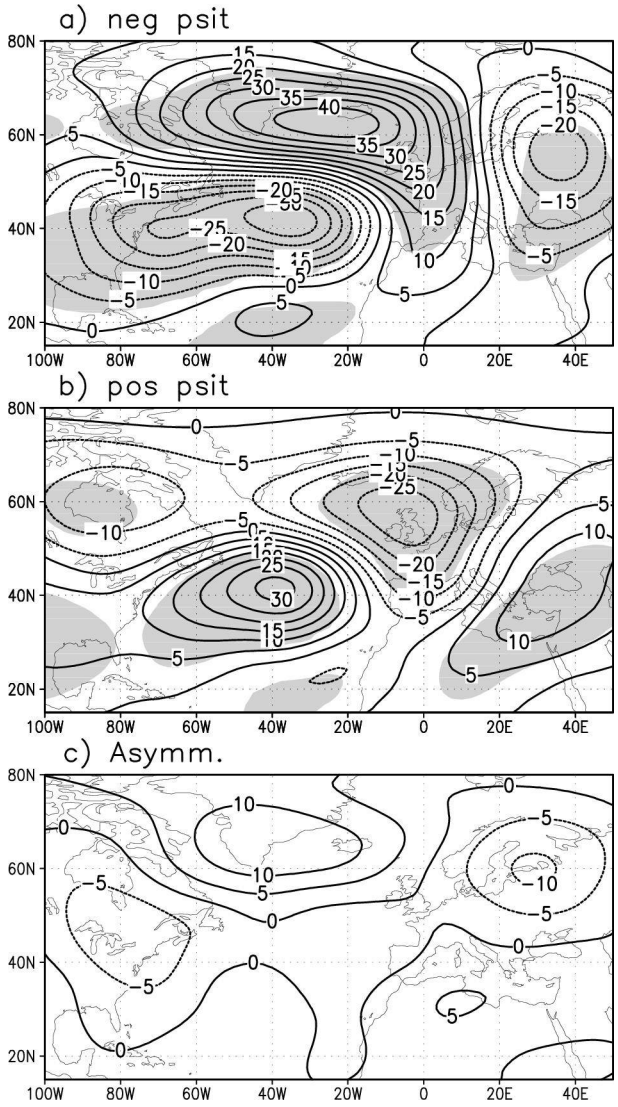

Fig.10 Composite of 500-hPa geopotential height anomaly for the months in February-April when the transient forcing anomaly around the Atlantic jet exit (40°W, 40°N) is strongly positive (a) and negative (b) in the control runs. (c) the antisymmetric component between (a) and (b). Unit: gpm. Shading is significant at the level of 95%.

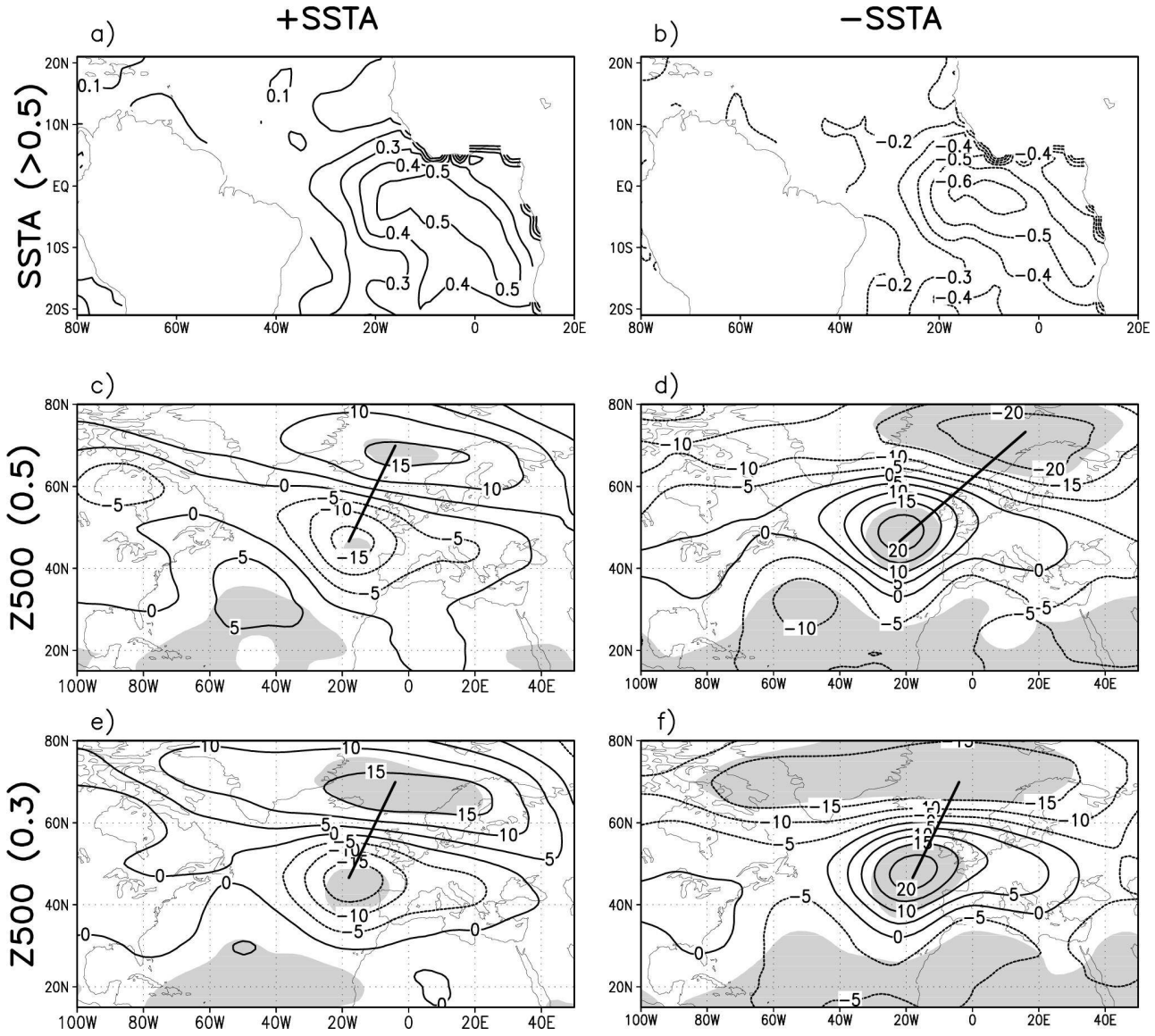

Fig. 11 Composite SSTA (a, b) (unit: ^{o}C) and 500-hPa geopotential heights (c, d) (unit: m) for the 53 positive and 49 negative SSTA months within October to December through 1948-1999 when the normalized SSTA projection coefficients on the tropical component of the Pan-Atlantic pattern are greater than 0.5 or less than -0.5. (e, f), as (c, d), but for the 63 positive and 61 negative SSTA months when the normalized projection coefficients are greater than 0.3 or less than -0.3. The thick solid line in (c-f) is the axis line of the height dipole for comparison. Shading in (c-f) is significant at the level of 90%.